

# Implementation of the FOPID algorithm in the PLC controller - PWR thermal power control case study

Bartosz Puchalski, Tomasz A. Rutkowski, Kazimierz Duzinkiewicz Faculty of Electrical and Control  
Engineering

Gdańsk University of Technology, G. Narutowicza Street 11/12, 80-233 Gdańsk, Poland

Email: bartosz.puchalski@pg.edu.pl, tomasz.adam.rutkowski@pg.edu.pl,

kazimierz.duzinkiewicz@pg.edu.pl

## Abstract

In the paper authors describe proposition of design and verification procedures of the discrete Fractional Order PID (FOPID) algorithm for control of the Pressurized Water Reactor (PWR) thermal power near its nominal operating point. The FOPID algorithm synthesis consists of: off-line optimal tuning of its parameters in continuous time-domain with LQ (Linear Quadratic) performance index and simplified models of nuclear reactor and control rods drive; its transformation into equivalent integer order structure with Oustaloup filters; and finally its transformation into equivalent discrete form. Discrete FOPID algorithm is further implemented in the PLC controller and verified by real-time simulation in the Hardware In the Loop (HIL) structure with non-linear nuclear reactor model. Promising simulation results were obtained, which confirm improved flexibility of the discrete FOPID algorithm in comparison to its classical PID counterpart.

## I. INTRODUCTION

Theory of the Fractional Order Calculus (FOC) involving, non-integer derivatives and integrals, is a well known field of study [1]. Methods based on FOC are willingly used in order to describe complex system dynamics and/or to achieve better control quality in various control systems [2], [3]. The Nuclear Power Plants (NPP) with PWR reactors are an example of such systems. There have been many recent publications presenting the usage of the FOC in modeling of processes occurring in nuclear reactor's cores [4], [5], [6] and for control purposes of such complex plants [7], [8], [9].

Nowadays more than 95% of the control loops in industry process control is based on classic PID (Proportional-Integral-Derivative) algorithm [10]. In most cases the integer order PID controllers are being used due to simplicity in implementation on digital platforms and due to well-known tuning methods. In order to enhance performance of the PID algorithm, in more complex and demanding applications, modifications in the structure of the algorithm can be introduced. In addition various techniques of parameter adaptation can be also introduced to the PID algorithm in order to control non-linear and non-stationary processes [11], [12], [13], [14], [15].

Despite various improvements in PID algorithms structure and tuning methodologies, all the above solutions have a subtle type of limitation, which is generally related to the integer order of integration and/or differentiation. A solution to this problem is the Fractional Order PID (FOPID) or  $PI^\lambda D^\mu$  algorithm [2]. The FOPID algorithm comes with two additional degrees of freedom related to integration ( $\lambda$ ) and differentiation ( $\mu$ ) order. Various types of digital and analog applications of the aforementioned FOPID controller with appropriate tuning and design methodologies may be found in the literature [16], [17]. The FOPID algorithm has also been introduced to the field of NPP control, for instance in the design of a fractional order phase shaper augmented with an optimal PID controller [18], robust fractional order PID controller [4] or fuzzy multi-regional controller with local  $PI^\lambda D^\mu$  controllers [9]. It has been shown that control algorithms which utilize fractional order operators prove to have better performance in terms of selected evaluation criteria, for instance ISE (Integral Squared Error) or LQ, in comparison to the integer order algorithms (PID) that were tuned with corresponding methods.

In the presented paper the authors focus on the optimal design, implementation and verification of the discrete FOPID algorithm for control of the PWR thermal power near its nominal operating point. Performance of the algorithm was verified by means of real-time simulation in the Hardware In the Loop (HIL) structure with non-linear PWR reactor model simulated in Matlab – SDRT environment [19], which cooperated with PLC controller where the designed discrete FOPID algorithm was implemented.

## II. PROBLEM STATEMENT

The NPPs are complex objects with non-linear processes dynamics with various time scales [20]. They are also classified as critical infrastructure facilities, therefore control of its basic controlled quantity – thermal power, is not a trivial task. Typically a classical SISO control system, presented on Figure 1 with conventional PID controller is used for that purpose. Every effort related to the improvement of the control system efficiency, for instance by introducing additional degrees of freedom in the form of integral and/or differential operators is greatly desired.

In the paper, authors describe discrete version of the FOPID algorithm design procedure, for the PWR reactor thermal power control purpose. It consists of four main steps presented on the Figure 2. At the beginning, the continuous FOPID algorithm is subjected to an off-line optimization task in the time-domain according to the LQ criterion. This task is performed using a simplified nuclear reactor model linearized in operation point that is related to the nominal working conditions of the PWR reactor – 100% of generated thermal power. Then, fractional order integral and differential operators, with parameters obtained from optimization are approximated with integer order

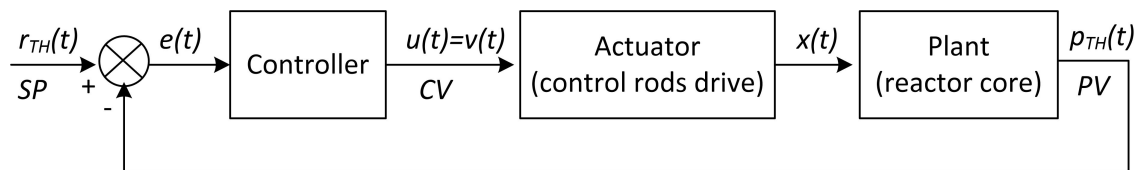


Fig. 1. Typical control system structure for reactor thermal power control where:  $r_{TH}(t)$ ,  $p_{TH}(t)$  - reference (SP) and realized (PV) reactor thermal power trajectory,  $e(t)$  - error signal,  $u(t)$  - control signal (CV) in the form of control rods velocity,  $x(t)$  - control rods immersion into the reactor core.



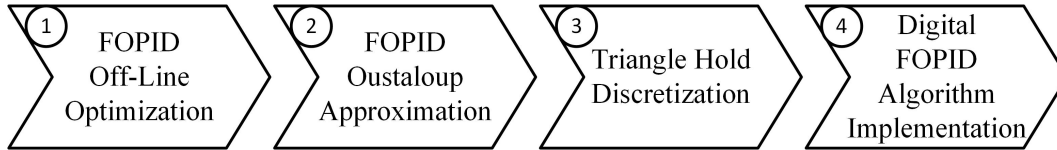


Fig. 2. Main steps of discrete FOPID algorithm design procedure.

continuous Oustaloup filters [21] in frequency-domain. Suitable Oustaloup filter parametrization related to selection of the appropriate order and frequency band, guarantee its adequate frequency characteristic which is compatible with the identified process dynamics and fractional order operators. After that, the Triangle Hold discretization method [22] is applied to the FOPID algorithm. As a result of this operation a discrete structure of the FOPID algorithm is obtained. This structure is easily implemented in the PLC controller with a high level Structured Text (ST) language [23] for instance with Simulink PLC Coder toolbox [24]. Finally, digital FOPID algorithm is verified via simulation tests in the Hardware In the Loop (HIL) structure. For HIL simulation tests purposes the multi-nodal, non-linear simulation model of PWR reactor was implemented in Simulink Desktop Real-Time (SDRT) toolbox [19]. This toolbox allows to simulate wide range of virtual objects in real-time regime on Personal Computer (PC). In HIL structure, the multi-nodal PWR reactor model, implemented on PC, cooperates via analog I/O acquisition boards with designed FOPID algorithm implemented in industrial PLC controller.

### III. RESEARCH METHOD

#### A. Plant models

The mathematical models of the processes occurring in the PWR reactor may be divided into two main groups, the first one is related to complex and accurate models, while the second one represents less accurate, reduced and simple models [20], [25], [26]. In this paper two such models of PWR nuclear reactor core are used for different purposes. Firstly the simplified linearized PWR reactor model is used for proposed FOPID control algorithm synthesis stage (*ModelA*). This model is a result of simplification of the multi-nodal model. Secondly the multi nodal, non-linear complex PWR reactor model (*ModelB*) [25], [26] is used for the HIL simulations that are related to control algorithm verification stage. The concept of the multi-nodal model is shown on Figure 3.

The multi-nodal PWR reactor model presented on Figure 3 is built based on the following components [25], [26]: (i) point kinetics model of nuclear reactor core used to describe the time-dependend average neutron density, including six groups of delayed neutrons; (ii) heat transfer model with two coolant nodes (odd and even respectively) assigned to each  $i$ -th distinguished fuel node; (iii) reactivity feedbacks due to changes in the fuel and coolant temperature; (iv) reactivity feedback due to the control rod bank movements; (v) and the assumption that the thermal power generated in the reactor core is proportional to the neutron flux and the average neutron density.

The multi-nodal reactor model (*ModelB*), consists of five fuel nodes and ten coolant nodes. Its simplified version (*ModelA*) is characterized by, one average delayed neutron precursor group, one fuel node ( $i = 1$ ), two coolant nodes and thermal power distribution coefficient equal to 1 ( $D_{Ci} = 1$ ).



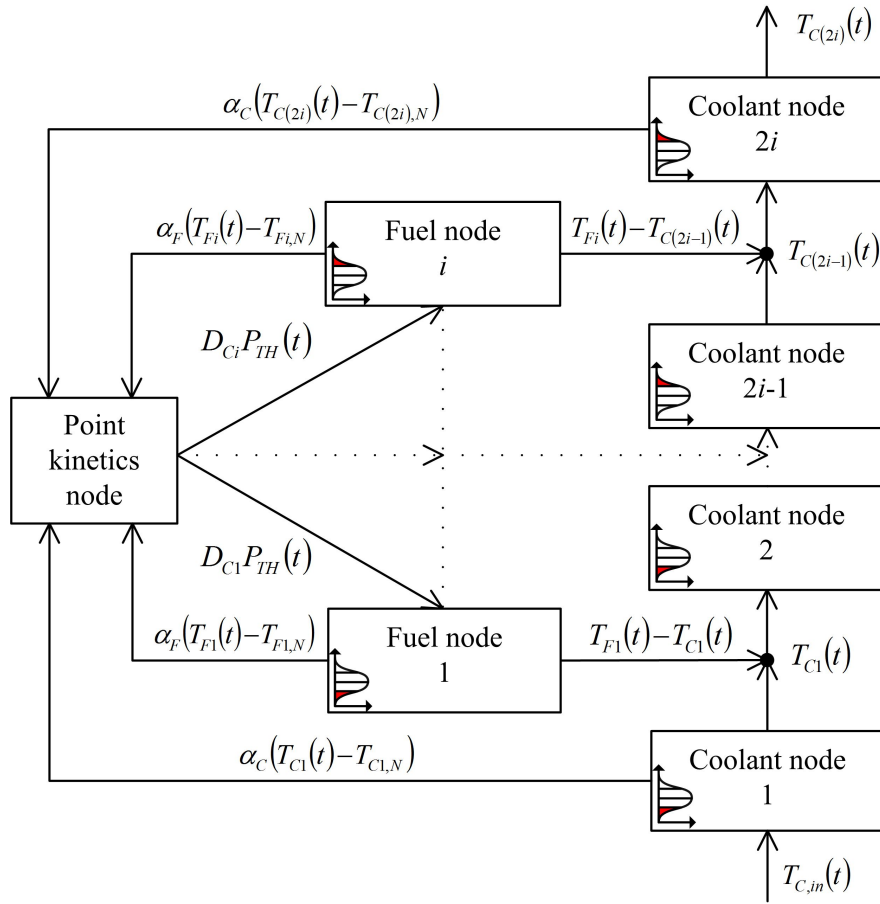


Fig. 3. Multi-nodal nuclear reactor core model structure, where:  $P_{TH}(t)$  - reactor thermal power,  $\alpha_F$  - fuel reactivity coefficient,  $\alpha_C$  - coolant reactivity coefficient,  $i$  - fuel node index,  $(2i - 1)$  - odd coolant node index,  $(2i)$  - even coolant node index,  $T_{F_i}(t)$  -  $i$ -th fuel node temperature,  $D_{C_i}$  - thermal power distribution coefficient for the  $i$ -th fuel node, play role of weight factors, which values are related to the depth  $x$  of control bank immersion into the reactor core,  $T_{C(2i)}(t)$  and  $T_{C(2i-1)}(t)$  - even and odd coolant nodes temperatures,  $T_{C,in}(t)$  and  $T_{C(2i)}(t)$  - coolant temperatures at inlet and outlet of reactor core.

In both models a non-linear control rods drive and control rods reactivity models are used

$$\frac{d\Delta\rho_{ext}(t)}{dx} = \frac{\rho_b}{\tilde{H}} \left( 1 - \cos\left(\frac{2\pi x}{\tilde{H}}\right) \right), \quad (1)$$

$$\frac{d\Delta\rho_{ext}(t)}{dt} = \frac{d\Delta\rho_{ext}(t)}{dx} \cdot \frac{dx}{dt}, \quad (2)$$

$$0 \leq x \leq \tilde{H}, \quad -1,9 \text{ cm/s} \leq \frac{dx}{dt} \leq 1,9 \text{ cm/s} \quad (3)$$

where  $\Delta\rho_{ext}$  describes the deviation of the external reactivity from its initial, critical value ( $\Delta\rho_{ext}(0) = 0$ ),  $\rho_b$  denotes control rods reactivity worth when they are fully immersed into reactor core,  $\tilde{H}$  denotes the reactor core height. Initial immersion of the control rods  $x(0)$  into reactor core is equal to 30% of  $\tilde{H}$ . Due to restrictions related to the size of this conference paper the authors did not describe parameters and equations of *ModelA* and *ModelB*.

All mentioned PWR reactor models (*ModelA*, *ModelB*) descriptions with parameters values may be found in the following publications [25], [26].

### B. FOPID algorithm design

In the field of automatic control the Grunvald-Letnikov definition [1], [2], [3] of the continuous integro-differential operator is widely used

$${}_a\mathfrak{D}_t^r f(t) = \lim_{h \rightarrow 0} h^{-r} \sum_{m=0}^{\lceil \frac{t-a}{h} \rceil} (-1)^m \binom{r}{m} f(t - mh), \quad (4)$$

where  $a$  and  $t$  are the limits of the operation,  $r$  denote the order of the operation. For  $r > 0$  the operator describes differentiation and for  $r < 0$  integration. Based on this definition, the FOPID algorithm may be presented in the continuous time-domain as follows

$$u(t) = K_P \cdot e(t) + K_I \cdot {}_0\mathfrak{D}_\infty^{-\lambda} e(t) + K_D \cdot {}_0\mathfrak{D}_\infty^\mu e(t) \quad (5)$$

where  $\lambda$  and  $\mu$  are nonnegative real numbers ( $\lambda, \mu \geq 0$ ),  $K_P$  denote proportional gain,  $K_I$  and  $K_D$  denotes the integration and differentiation gains, respectively.

Intuitively, due to two additional parameters introduced in the FOPID controller comparing to the classical PID equivalent there are more degrees of freedom in adjusting overall control system performance. However, finding optimal set of values for those parameters, in order to meet the user specification for the given process, is not a trivial task. In the literature may be found various propositions for FOPID algorithm tuning strategies, starting from empirical rules and ending with analytical techniques [3]. In the paper the optimal tuning methodology for FOPID algorithm has been proposed. Optimal values of FOPID parameters are the solution of a optimization task defined below in the continuous time-domain with LQ integral quality criterion

$$\min_x f_{LQ} = \int_0^t (e^2(x, \tau) + u^2(x, \tau)) d\tau, \quad \text{st.} \quad (6)$$

$$x = [K_P, K_I, \lambda, K_D, \mu] \text{ and } x \geq 0, \quad (7)$$

$$|\arg(p_j)| > \alpha \cdot \frac{\pi}{2}. \quad (8)$$

In the optimization problem summarized by formulas (6)-(8) symbols  $e$  and  $u$  represent the error and control signal as shown on Figure 1. Optimization task utilizes linear models of both the plant (*ModelA*) and the control rods drive – actuator. Therefore, the entire model of the control system (Figure 1) used in the optimization task consisted of linear elements. Hence, in the optimization task a unit step reference thermal power trajectory was used.

The stability of the controlled system is guaranteed in the optimization process by the inequality constraint described by formula (8). Using this constraint, it is examined whether the poles  $p_j$  of the corresponding commensurate-order [3] closed-loop control system are in the appropriate region of the complex plane. The commensurate-order transfer function of the corresponding fractional order system is defined as

$$G(\delta) = \frac{b_1\delta^m + b_2\delta^{m-1} + \dots + b_m\delta + b_{m+1}}{a_1\delta^n + a_2\delta^{n-1} + \dots + a_n\delta + a_{n+1}}, \quad (9)$$

where  $\delta = s^r$ , and  $r$  is chosen herein as equal to 0,001.

For comparison purposes, corresponding optimization task has been carried out for the classic version of the PID controller with parameters  $K_P$ ,  $K_I$ ,  $K_D$ . In this case the constraint (8) correspond to the classical version of the stability of the LTI systems where all poles of the closed-loop control system must be located in complex LHP. The off-line optimization results for FOPID and PID controllers are presented in Table I. Mesh Adaptive Direct Search [27] algorithm with additional search step that utilized Genetic Algorithm [28] was used to solve the optimization task (6)-(8).

TABLE I  
OPTIMIZATION RESULTS

Controller	$K_P$	$K_I$	$\lambda$	$K_D$	$\mu$	$f_{LQ}$
PID	1,284	0,036	n/a	0,000	n/a	1,400
FOPID	0,186	1,076	0,161	0,028	0,543	1,383

### C. FOPID algorithm approximation with Oustaloup filter

The numerical procedures typically used to evaluate fractional order integral and differential operators are not useful, due to their complexity and the need for infinite memory resources. Therefore implementation of the FOPID controller on PLC platform is impossible using typical FOC numerical procedures. The authors propose to approximate the fractional order operators  $\mathfrak{D}^{-\lambda}$  and  $\mathfrak{D}^{-\lambda}$  of the optimally designed continuous FOPID algorithm with integer order continuous Oustaloup filters  $G_O^{-\lambda}(s)$  and  $G_O^\mu(s)$  adjusted in the frequency-domain

$$G_O^{-\lambda,\mu}(s) = K_P + K_I \cdot G_O^{-\lambda}(s) + K_D \cdot G_O^\mu(s). \quad (10)$$

The single Oustaloup filter [21] is defined as a frequency-band real non-integer differentiator, with fractional order  $\alpha$  and frequency-band in the range  $\omega \in \langle \omega_b, \omega_h \rangle$  as follows

$$G_O^\alpha(s) = \left( \frac{\omega_u}{\omega_h} \right)^\alpha \left( \frac{1 + \frac{s}{\omega_b}}{1 + \frac{s}{\omega_h}} \right)^\alpha, \quad (11)$$

where  $\omega_u$  denote the unit gain frequency ( $\omega_u = \sqrt{\omega_b\omega_h}$ ) and  $\alpha \in R$ . Oustaloup [21] proposed the approximation of non-integer order filter (11) with integer order filter, which real zeros  $\omega'_k$  and poles  $\omega_k$  are recursively distributed over the complex plane. Transfer function of the integer order Oustaloup filter takes the following form [3]

$$G_O^\alpha(s) = \lim_{N \rightarrow \infty} G_{O,N}^\alpha(s) = \lim_{N \rightarrow \infty} \omega_h^\alpha \prod_{k=-N}^N \frac{s + \omega'_k}{s + \omega_k} \quad (12)$$

where  $\alpha$  is the order of the fractional operator.

Aforementioned Oustaloup filter definition avoids the restriction on  $\omega_b\omega_h = 1$  so the frequency boundaries can be selected independently [3]. The parametrization of Oustaloup filters  $G_O^{-\lambda}(s)$  and  $G_O^\mu(s)$ , must be done according

to the appropriate filters orders  $(2N + 1)$  and frequency band  $\omega \in \langle \omega_b, \omega_h \rangle$ . Appropriate parametrization guarantee adequate frequency characteristics of the filters which takes into account dynamics of the considered plant and fractional order operators. Frequency band of the plant was identified with respect to the lowest/highest real values of the zeros and poles of the linearized *ModelA* and it is within the range of frequencies  $\langle \omega_A, \omega_B \rangle$  given in Table II. To obtain a correct approximation of the fractional operators with the Oustaloup filters the frequency boundaries of the filters  $\langle \omega_b, \omega_h \rangle$  must satisfy the following conditions [21]:  $\omega_b \ll \omega_A$ ,  $\omega_h \gg \omega_B$ . The final parameters of the Oustaloup filters have been listed in Table II.

TABLE II  
OUSTALOUP FILTERS PARAMETERS

$\omega_b$ [rad/s]	$\omega_h$ [rad/s]	$\omega_A$ [rad/s]	$\omega_B$ [rad/s]	$N$
0,0006095	36283,35	0,06095	362,8335	4

#### D. FOPID algorithm discrete representation

During implementation of any control law in the PLC controller it is necessary to take into consideration following aspects: (i) controller sweep time, which should be constant and adjusted with respect to the fastest time constant identified in the controlled process; (ii) control algorithm representation should be described in a way, which allows direct implementation with one of the PLC programming languages; (iii) algorithm computational time should allow its execution in finite and predetermined period. In the last case the sweep time of the PLC controller should be considered as constraint during algorithm synthesis and implementation.

In the case of fractional order control algorithm implementation, the description presented previously in subsections III-B and III-C is still problematic for direct implementation in PLC controller. For that purpose the discrete control algorithm representation is needed. In the literature may be found several methods for fractional systems direct discretization e.g. PSE (Power Series Expansions) or CFE (Continuous fractional Expansions) [3]. In the paper the authors propose to use the Triangle Hold discretization method [22]. It is applied to the controller structure with the integer order Oustaloup filters (10). Finally, the FOPID controller structure may be presented in the discrete state space form. That form of control algorithm description allows its easy implementation in PLC controller with e.g. structural text language (ST) [23] using typical data structures such as vectors, basic arithmetic operations such as addition, subtraction, multiplication and division, basic repetition control structure in the form of FOR-loop and repeating cycle nature of user program execution in PLC device

During algorithm verification stage the authors observed that proposed discretization method guarantee satisfactory quality of continuous systems approximation in frequency-domain, and its discrete representation with a minimal set of parameters in the form of rational numbers in comparison to other popular discretization methods.

According to the Table II, the largest time constant present in a nuclear reactor model is related to frequency  $\omega_B = 362,83$  rad/s. Taking into account Nyquist's theorem, the digital control algorithm should sample data at a frequency minimally twice as high as the highest time constant in the model. Therefore, the PLC controller sweep

time should be set to a minimum value of approx. 8 ms. The minimum sweep time that could be achieved on the PLC controller used in this study was equal to 9 ms. Although the required sweep time was not achieved, the implemented FOPID algorithm was capable of effective control of the thermal power of a nuclear reactor as presented in section IV.

#### IV. RESULTS

The discrete FOPID algorithm presented in the article has been subjected to simulation tests carried out with the usage of *ModelB*. The simulations were carried out in two different environments. Firstly, overall control system structure presented on Figure 1 was simulated in the Matlab/Simulink rapid prototyping environment – subsection IV-A. Secondly, simulation tests in the HIL structure presented on Figure 4 were performed and described in subsection IV-B. HIL structure is characterized by the separation of the control algorithm, in this case implemented in the PLC controller, from the plant, which in this instance is implemented in the real-time environment. In both cases the same stepwise trajectory was used which was supposed to cause the control system under consideration to deviate from nominal point by  $\pm 5\%$ .

##### A. Software simulation results

In this subsection results regarding comparison between different realizations of the FOPID algorithm in the software simulation environment (Matlab/Simulink) are shown. During the simulation tests, the integrator windup effect which reduces the quality of control was observed for the FOPID controllers. To overcome this effect the appropriate Back-Calculation Anti-Windup strategy [10] was applied to the FOPID algorithm with feedback gain  $K_B = 1/T_t$  set to 2.61. The analogous Anti-Windup strategy was introduced to the PID/FOPID controller implemented in the PLC controller which was tested in HIL structure. The  $K_B$  gain for PID controller was set to 0.05.

On Figure 5 responses of the considered in the paper control system with different realizations of FOPID algorithm are shown. The blue dashed line represent given set point (SP) trajectory of the PWR reactor thermal power. The red and the yellow lines represent responses of the control system with FOPID algorithm which has been implemented using continuous Oustaloup filters and discretized Oustaloup filters, respectively. On this figure the response of the

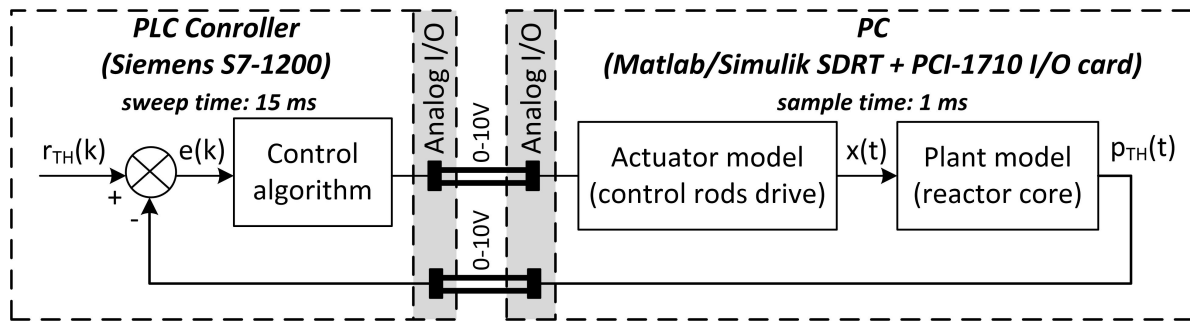


Fig. 4. Hardware In the Loop (HIL) structure.



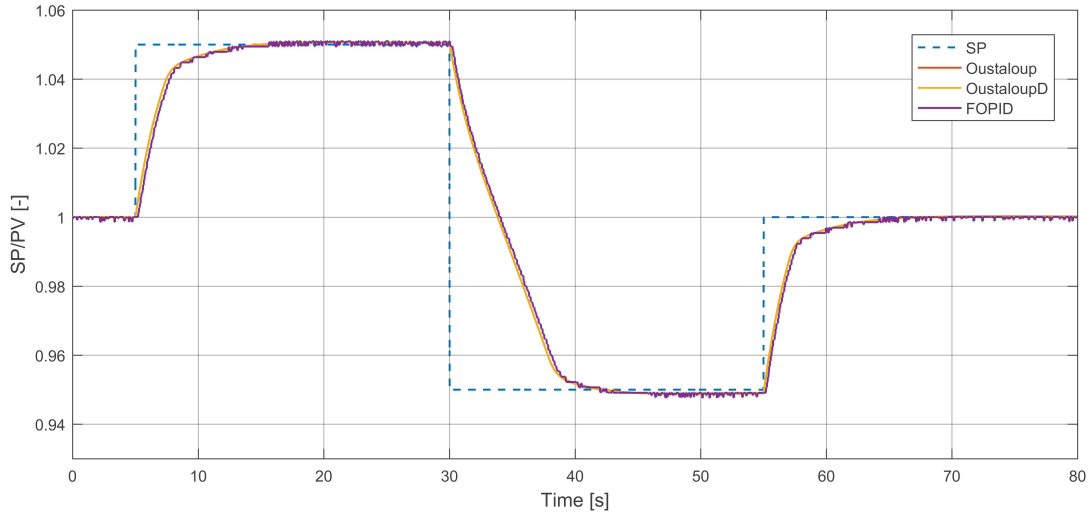


Fig. 5. Comparison of stepwise trajectory tracking between FOPID algorithms with Anti-Windup strategy tested in software simulation environment and HIL structure.

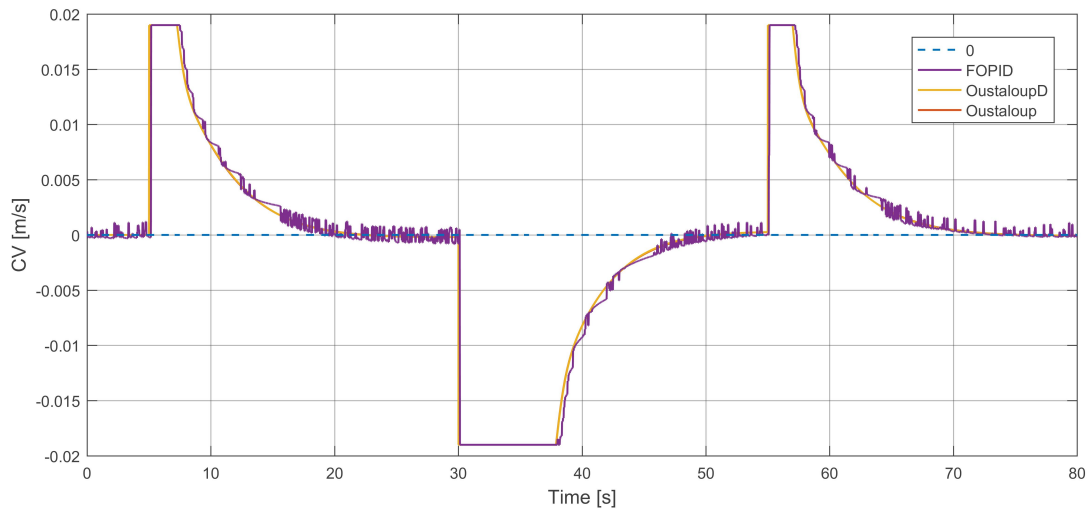


Fig. 6. Comparison of control signals generated by FOPID algorithms with Anti-Windup strategy tested in software simulation environment and HIL structure.

HIL control system with the discretized FOPID algorithm implemented on PLC controller has also been plotted with violet line for comparison.

On Figure 6 the control signals from different realizations of FOPID algorithm are presented. The blue dashed line represents control signal equal to 0 m/s. Other colors on that figure has similar meaning as on the Figure 5.

As expected, presented simulation tests results show that different implementations (continuous, digital) of the FOPID algorithm yield the same results, which indicates the correct design and implementation of discrete FOPID algorithm. The analysis of Figure 6 shows that the control signal from the controller operating in the HIL structure

is noisy which was also to be expected because of the physical, analog connections between the elements present in this structure. Despite the noise, the nature of this signal is similar to the reference signals generated by continuous and discrete implementations of the FOPID controller.

### B. Hardware In the Loop simulation results

In this subsection results regarding comparison between different types of discrete PID and FOPID algorithms tested in the HIL structure are shown.

In this case, on Figure 7 responses of the considered control system structure (Figure 4) with various types of discrete PID and FOPID algorithms implemented in the PLC controller are presented. As previously, the blue dashed line represents given set point (SP) trajectory of the desired PWR reactor thermal power. The red and the yellow lines represents responses of the control system with discrete PID algorithms which were provided by the manufacturer of the PLC controller. Those algorithms were tuned by automatic tuning procedures provided by the manufacturer. The red line corresponds to the PID algorithm tuned according to the simplified procedure (PreTuning), the yellow line corresponds to the PID algorithm tuned using the more accurate tuning method (FineTuning). While the violet and the green lines corresponds to the control system with discrete FOPID and PID algorithms, which were tuned based on the optimization procedure presented in the subsection III-B. The PreTuning procedure provided by the PLC manufacturer is based on the open-loop step response method [10]. On the other hand the FineTuning procedure provided by the PLC manufacturer is based on the closed-loop Relay-Method [10]. On Figure 8 the control signals from various types of PID and FOPID algorithms in HIL structure are shown. The blue dashed line represents control signal equal to 0 m/s. The red and the yellow lines, as on previous figures, represents control signals from PID algorithms, which were provided by the manufacturer of the PLC controller. As in previous figure the violet and the green lines corresponds to control signals from FOPID and PID algorithms, respectively.

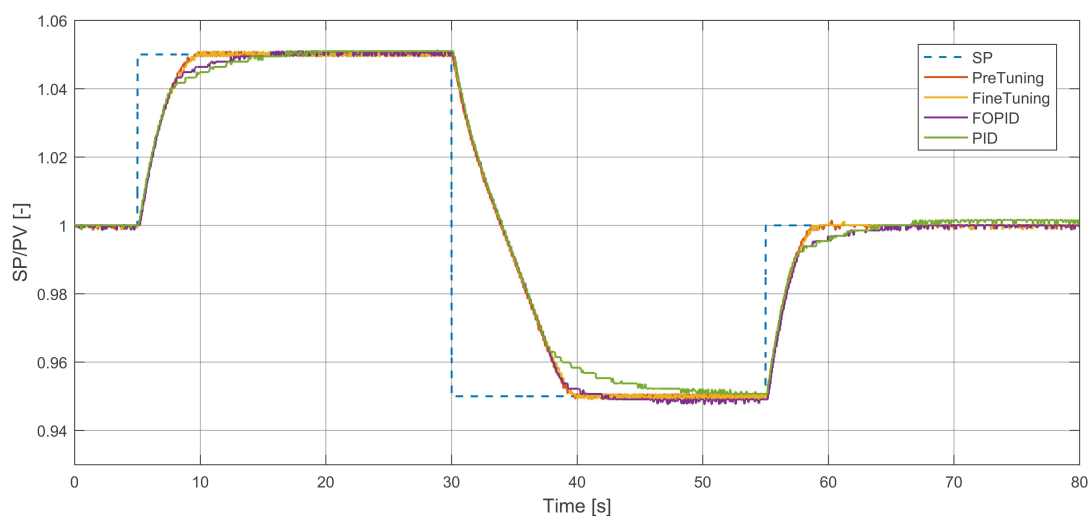


Fig. 7. Comparison in stepwise trajectory tracking between different types of PID algorithms and FOPID algorithm working in HIL structure.

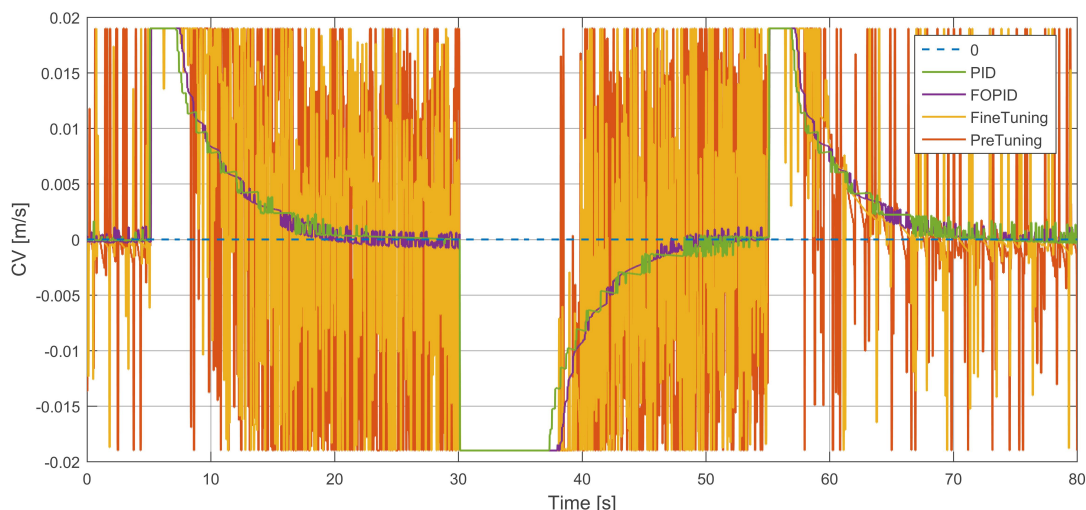


Fig. 8. Comparison in control signals generated from different types of PID algorithms and FOPID algorithm working in HIL structure

Presented results show that PID algorithms provided by the manufacturer of the PLC controller are characterized by the best tracking of the demanded thermal power trajectory. Despite this fact they cannot be considered as proper due to the very high noise level of the generated control signal. On the other hand FOPID controllers with applied Anti-Windup strategy which were tuned with the procedure presented in this article do not differ significantly from the PID controllers provided by the manufacturer. Their advantage is clearly visible in the control signals which are far less noisy. The classical PID controller was the worst of the controllers that participated in this study due to poor reference trajectory tracking.

## V. CONCLUSIONS

In the article the method of implementation of the FOPID algorithm on the PLC platform was presented. Presented method of implementation was verified in the HIL environment using a complex PWR reactor model. Verification phase proved that the implemented FOPID algorithm is comparable to the PID controller proposed by the PLC manufacturer in trajectory tracking. It should be clearly stated that both algorithms were tuned with completely different methods. It is also important to state that the presented FOPID algorithm outperformed the PLC manufacturer PID controller in terms of less noisy control signal. The main drawback, identified by the authors, is related to computational complexity of the FOPID controller. Presented approach allows to obtain a very good representation of fractional order operators. Despite the effort spent on implementation, the use of the FOPID controller result in an improvement in the control quality especially in comparison to the classical PID approach tuned with the corresponding method. At present, there are very few articles related to the problem of implementation of fractional order controllers on the basic digital control platform used in industry, namely the PLC controller. The authors believe that this article is an important contribution related to research on the possibilities of implementing control algorithms based on fractional order operators on modern digital platforms,

i.e. PLC controllers. In particular, it shows a case in which a very complex plant, such as a PWR reactor, has been taken into account.

## ACKNOWLEDGEMENTS

The research work was done under grant Polish MNiSW 8902/E – 359/M/2017: Young Researcher Support Program. The authors wish to express their thanks for support.

## REFERENCES

- [1] K. B. Oldham and J. Spanier, *The fractional calculus: theory and applications of differentiation and integration to arbitrary order*. Dover Publications, 2006.
- [2] I. Podlubny, *Fractional differential equations*. Elsevier, 1998, vol. 198.
- [3] D. Xue, *Fractional-order Control Systems: Fundamentals and Numerical Implementations*. Walter de Gruyter GmbH & Co KG, 2017, vol. 1.
- [4] S. Das, S. Das, and A. Gupta, "Fractional order modeling of a PHWR under step-back condition and control of its global power with a robust  $PI^\lambda D^\mu$  controller," *IEEE Transactions on Nuclear Science*, vol. 58, no. 5, pp. 2431–2441, 2011.
- [5] T. K. Nowak, K. Duzinkiewicz, and R. Piotrowski, "Fractional neutron point kinetics equations for nuclear reactor dynamics—numerical solution investigations," *Annals of Nuclear Energy*, vol. 73, pp. 317–329, 2014.
- [6] —, "Numerical solution analysis of fractional point kinetics and heat exchange in nuclear reactor," *Nuclear Engineering and Design*, vol. 281, pp. 121–130, 2015.
- [7] S. Das, I. Pan, and S. Das, "Fractional order fuzzy control of nuclear reactor power with thermal-hydraulic effects in the presence of random network induced delay and sensor noise having long range dependence," *Energy Conversion and Management*, vol. 68, pp. 200–218, 2013.
- [8] B. Puchalski, K. Duzinkiewicz, and T. Rutkowski, "Analiza sterowania ułamkowego  $PI^\lambda D^\mu$  mocą reaktora jądrowego," *Informatyka, Automatyka, Pomiar w Gospodarce i Ochronie Środowiska*, no. 4, pp. 63–68, 2013.
- [9] —, "Wieloobszarowa rozmyta regulacja  $PI^\lambda D^\mu$  mocy reaktora jądrowego," in *Aktualne Problemy Automatyki i Robotyki*, K. Malinowski, J. Józefczyk, and J. Świątek, Eds. Akademicka Oficyna Wydawnicza EXIT, 2014, vol. 20, pp. 544–557.
- [10] K. J. Åström and T. Hägglund, *PID controllers: theory, design, and tuning*. Instrument society of America Research Triangle Park, NC, 1995, vol. 2.
- [11] Z.-Y. Zhao, M. Tomizuka, and S. Isaka, "Fuzzy gain scheduling of PID controllers," *IEEE transactions on systems, man, and cybernetics*, vol. 23, no. 5, pp. 1392–1398, 1993.
- [12] B. Puchalski, K. Duzinkiewicz, and T. Rutkowski, "Multi-region fuzzy logic controller with local PID controllers for U-tube steam generator in nuclear power plant," *Archives of Control Sciences*, vol. 25, no. 4, pp. 429–444, 2015.
- [13] B. Puchalski, T. Rutkowski, J. Tarnawski, and K. Duzinkiewicz, "Comparison of tuning procedures based on evolutionary algorithm for multi-region fuzzy-logi PID controller for non-linear plant," in *Methods and Models in Automation and Robotics (MMAR), 2015 20th International Conference on*. IEEE, 2015, pp. 897–902.
- [14] P. Sokółski, T. A. Rutkowski, and K. Duzinkiewicz, "The excitation controller with gain scheduling mechanism for synchronous generator control," in *Methods and Models in Automation and Robotics (MMAR), 2015 20th International Conference on*. IEEE, 2015, pp. 23–28.
- [15] P. Sokółski, K. Kulkowski, A. Kobylarz, K. Duzinkiewicz, T. Rutkowski, and M. Grochowski, "Advanced control structures of turbo generator system of nuclear power plant," *Acta Energetica*, vol. 3, no. 24, pp. 83–90, 2015.
- [16] A. Soukkou, M. Belhour, and S. Leulmi, "Review, design, optimization and stability analysis of Fractional-Order PID controller," *International Journal of Intelligent Systems and Applications*, vol. 8, no. 7, p. 73, 2016.
- [17] S. Das, I. Pan, S. Das, and A. Gupta, "A novel fractional order fuzzy PID controller and its optimal time domain tuning based on integral performance indices," *Engineering Applications of Artificial Intelligence*, vol. 25, no. 2, pp. 430–442, 2012.
- [18] S. Saha, S. Das, R. Ghosh, B. Goswami, R. Balasubramanian, A. Chandra, S. Das, and A. Gupta, "Design of a fractional order phase shaper for iso-damped control of a PHWR under step-back condition," *IEEE Transactions on Nuclear Science*, vol. 57, no. 3, pp. 1602–1612, 2010.
- [19] MathWorks, "Simulink Desktop Real-Time," March 2018. [Online]. Available: <https://www.mathworks.com/products/simulink-desktop-real-time.html>
- [20] J. J. Duderstadt and L. J. Hamilton, *Nuclear reactor analysis*. Wiley New York, 1976, vol. 1.
- [21] A. Oustaloup, F. Levron, B. Mathieu, and F. M. Nanot, "Frequency-band complex noninteger differentiator: characterization and synthesis," *IEEE Transactions on Circuits and Systems I: Fundamental Theory and Applications*, vol. 47, no. 1, pp. 25–39, 2000.



- [22] G. F. Franklin, J. D. Powell, and M. L. Workman, *Digital control of dynamic systems*. Addison-wesley Menlo Park, CA, 1998, vol. 3.
- [23] K. H. John and M. Tiegelkamp, *IEC 61131-3: Programming Industrial Automation Systems*. Springer Science & Business Media, 2010.
- [24] MathWorks, “Simulink PLC Coder,” March 2018. [Online]. Available: <https://www.mathworks.com/products/sl-plc-coder.html>
- [25] B. Puchalski, T. A. Rutkowski, and K. Duzinkiewicz, “Multi-nodal PWR reactor model—methodology proposition for power distribution coefficients calculation,” in *Methods and Models in Automation and Robotics (MMAR), 2016 21st International Conference on*. IEEE, 2016, pp. 385–390.
- [26] —, “Nodal models of pressurized water reactor core for control purposes—a comparison study,” *Nuclear Engineering and Design*, vol. 322, pp. 444–463, 2017.
- [27] C. Audet and J. E. Dennis Jr, “Mesh adaptive direct search algorithms for constrained optimization,” *SIAM Journal on optimization*, vol. 17, no. 1, pp. 188–217, 2006.
- [28] D. E. Goldberg, *Genetic Algorithms in Search, Optimization and Machine Learning*, 1st ed. Boston, MA, USA: Addison-Wesley Longman Publishing Co., Inc., 1989.